Acta of Bioengineering and Biomechanics
Vol. 19, No. 2, 2017

Original paper
DOI: 10.5277/ABB-00621-2016-03

Phase composition and morphology characteristics of ceria-stabilized zirconia powders obtained via sol-gel method with various pH conditions

DAMIAN S. NAKONIECZNY[1]*, ZBIGNIEW K. PASZENDA[1], MARCIN BASIAGA[1], TOMASZ RADKO[2], SABINA DREWNIAK[3], JACEK PODWÓRNY[4], WOJCIECH BOGACZ[5]

[1] Department of Biomaterials and Medical Devices Engineering, Faculty of Biomedical Engineering, Silesian University of Technology, Zabrze, Poland.
[2] Institute for Chemical Processing of Coal, Zabrze; Poland.
[3] Department of Optoelectronics, Silesian University of Technology, Gliwice, Poland.
[4] Refractory Materials Division, Institute of Ceramics and Buildings Materials, Gliwice, Poland.
[5] Department of Chemical Engineering and Process Design, Faculty of Chemistry, Silesian University of Technology, Gliwice, Poland.

Purpose: High purity, fine crystalline, degradation-free at low temperature powders have attracted special interest in CAD/CAM prosthetic dentistry full ceramic restorations. This study reports the preparation and characterisation of zirconia-ceria (0.9 ZrO_2 0.1 CeO_2) powders. Materials were obtained from zirconium-n-alkoxide and cerium nitrate hexahydrate in the pH 2–4 and 8–10. *Methods:* Zirconia-ceria powders were obtained with the sol-gel method in a humid-free environment. Thermal analysis (TGA/DTA) of the as-prepared materials was made for an assessment of its behaviour at elevated temperatures. Specimens were dried at 80 °C and calcinated in two stages: at 300 °C with soaking time 2.5 h and 850 °C with holding time 2.5 h, in order to evaluate the phase transformations. Thermal analyses of the as-dried powders were made for an assessment of its thermal behaviour during heat treatment up to 1000 °C. By X-ray diffraction (XRD), polymorphs of ZrO_2 were identified. Additionally, scanning electron microscopy (SEM) and laser particle size distribution (PSD) were involved for characterisation of morphology of the powders. *Results:* A correlation between the pH of the colloidal system and the morphology of the as-obtained powders were found. Based on analysis (SEM, PSD), structures were identified known as soft and hard agglomerates. *Conclusions:* It can be stated that differences found between powder morphology were dependent on the value pH used, which can be crucial for powder densification during sintering and compacting green bodies which, as a consequence, may be crucial for the lifetime of zirconia prostheses. Correlations between phase composition and pH are difficult to grasp, and require further, more sophisticated, studies.

Key words: *sol-gel, bioceramics, zirconia, oxide dopants, thermal properties, powder morphology*

1. Introduction

Zirconium oxide stabilised with yttrium oxide (YSZ) is a commonly used material for making fixed dentures such as crowns, bridges, posts, implants and veneering ceramics with aesthetics comparable to the best effects obtained with composites used in preventive dentistry [13], [17], [25]. A controversial issue associated with the use of zirconium oxide in dental prosthetics is the martensitic transformation of the tetragonal phase *t*-ZrO_2 to monoclinic *m*-ZrO_2, accompanied by an increase in the grain volume [3]. The transformation standby from the surface and continues into the interior of the restoration, resulting in a significant increase of internal stresses that may ultimately lead to the destruction of the prosthesis, increasing the cost of the treatment [3]. Therefore, it can be stated that the transformation $t \rightarrow m$ is a key factor that is beneficial and crucial to the properties and the

* Corresponding author: Damian Nakonieczny, ul. Charlesa de Gaulle'a 40, 41-800 Zabrze, Poland. Tel: +48 0791515766, email: damian.nakonieczny@polsl.pl
Received: April 14th, 2016
Accepted for publication: June 30th, 2016

lifetime of the ceramic restoration. The phase transition favours the aging of the material and its degradation. The aging process of the material occurs at moderate temperatures below 400 °C and is found to be most rapid over the temperature range between 200–300 °C [10]. Additional factors that accelerate the aging are mechanical stress, prosthesis laboratory treatment and interactions with electrolytes in the human oral cavity and body fluids [10], [14]. Adverse changes occurring are the so-called *low-temperature degradation* (*LTD*) and, to the best of current knowledge, they are still an unsolved problem that has been the subject of numerous investigations [1], [7], [10]. The mechanism of the transformation has been correctly described by Guo, who noted that the kinetics of transformation is strongly dependent on the occurrence of O^{2-} vacancies [9]. The kinetics of these changes can be described by the dependence derived by Mehl–Avrami–Johnson (MAJ) [15]. LTD is an autocatalytic process that is substantially irreversible at a body temperature environment. Based on the Guo and Chevalier's research, it can be clearly concluded that the most significant impact on the problem of stabilisation and LTD resistance of β-ZrO_2 is a type and concentration of oxide stabiliser, the value of the ceramic matrix Young's modulus, and the grain size [7], [9]. These variables have an impact on the susceptibility to phase transformation between tetragonal and monoclinic grains [7]. Therefore, an issue of stabilising additives is essential to obtain LTD-insensitive ceramics for dental applications. Based on many years of research, it was found that the best stabilising additives of metastable phases are metal oxides [3]. Oxides suitable for stabilising metastable phases fall into the scandium and lanthanides groups. Also appropriate can be yttrium and cerium oxide. The most important factors that should to be taken into account in the selection of the stabiliser are: the radius of the Me^{n+} cation, the valence state of the cation, the amount of the introduced O^{2-} vacancies, and the distortion of the crystal lattice caused by the introduction of the dopant [3]. Additives whose cation radius is greater than Zr^{4+} favour the stabilisation of metastable phases. The valence of the cation has an influence on stabilisation achieved. It is also worth noting that a very good stability can be achieved by multi-oxide systems. Additionally, with the increase of the vacancies' concentration in the zirconia lattice, the stability of metastable phases is improved. Dopant cations with a coordination number less than Zr^{4+} are desirable. Distortion of the crystal lattice occurring after the introduction of stabilising agents changes the lattice parameters of matrix (*t*) and (*c*) phases, which may be beneficial for improving stability [5]. Other factors that influence the stability of the metastable phases are grain size and morphology of the as-obtained powders, which allow solid green bodies to be prepared [4]. The influence of the grain size is discussed in almost every paper concerning doping and stabilisation of ZrO_2 [2]. The effect of grain size is now relatively well understood. Grain size is dependent on valence state and concentration of the stabilizer, and has a major impact on the phase composition [20]. In addition, it should be noted that with increasing grain size the martensitic transformation temperature decreases: the smaller the grain, the highest phase transformation temperature [12]. An important concern linked to heat treatment is growth of the grain during the heating: the grain growth rate depends mostly on the diffusion coefficient. Diffusion coefficients of metastable phases' are higher than those of the m-ZrO_2 grains, and therefore they are able to undergo LTD [19]. For these reasons, it can be clearly stated that zirconia ceramics for dental prosthetic treatment purposes should be characterised by grain sizes as small as possible, a single phase composition and, depending on the moisture destructive environment, an appropriately selected tetragonal phase stabilising agent. It is generally known that with the sol-gel method various materials including powders with strictly controlled chemical and phase composition, and the desired morphology can be obtained. Changing the solvent type, pH value, reaction temperature, molar ratios of reactants or type of the oxide precursors can affect the properties of the final ceramic [16], [19]. Studies are being performed, e.g., Caruso et al. [16], which deal with the correlations between synthesis parameters and the morphology of ceramic powders, and their subsequent properties during the preparation of green bodies, e.g., during sintering. As clearly indicated by the results obtained by Caruso et al. [16], the pH of a colloidal solution plays a significant role in porosity, green body compaction, tetragonal phase stabiliser distribution, grain size, degree of agglomeration, and also has a significant influence on the susceptibility to LTD of zirconia in the oral cavity environment. The aim of this study is to understand the mechanisms of sol-gel powder preparation and its influence on the thermal properties, phase composition and microstructure of the as-obtained cerium-doped zirconia powders. For these reasons, the main subject of this paper was the influence of pH of the solution during synthesis, and acetic, hydrochloric acids and ammonia addition to the aforementioned properties.

2. Materials and methods

2.1. Powder preparation

As a zirconia precursor we used zirconium n-propoxide (ZNP, 70% wt. in propanol, Sigma Aldrich). 2-propanol was used as a solvent (PrOH, Avantor). As a ceria precursor, cerium nitrate hexahydrate (CNH, 1M solution in 2-propanol, Sigma Aldrich) was used. To stabilise the sol and control the hydrolysis rate as a chelating agent Acetylacetone was used (AcAc, Avantor). To obtain the desired pH, acetic acid (CH_3COOH, Avantor), hydrochloric acid (HCl, Avantor) or ammonia (NH_4OH, Avantor) was used. Sample characterisation and reactants' molar ratios are shown in Table 1. For the reactant, we also used deionised water. All reagents were used without any further purification. The whole synthesis took place in a Shlenk-type round bottom flask with continous nitrogen flow. First, mix type of ZNP in PrOH was made. Then, in order to control the rate of hydrolysis rate, AcAc was added. After 1 hour of stirring, CNH solution in 2-propanol was added. Subsequently, depending on the calculated pH of CH_3COOH, HCl or NH_4OH was being added. All pH-agents were mixed with PrOH and carefully added to the flask. In the last sequence a deionised water also mixed with PrOH was added very carefully in a drop-by-drop way. After 2 hours of mixing, the as-obtained gel was shredded, and dried at 80 °C for 24 h in an ambient atmosphere. The resulting pre-calcined powders were ground with a pestle and mortar and calcined. Samples were calcined in an air atmosphere in a muffle furnace (Renfert Magma) in a two-stage heating process: first stage – heating rate of 9 °C/min, final temperature of 300 °C, holding time 1 h; second stage – heating rate of 9 °C/min, final temperature of 800 °C, holding time 1 h. The samples were cooled in a furnace chamber for the night. All powder preparation detailed stages are shown in a block diagram (Fig. 1).

Table 1. Sample characteristics

Sample	Molar Ratio ZNP:PrOH:H_2O:AcAc	pH-Agent	pH
A	1:2:2:0.194	–	6÷6.5
B1	1:2:2:0.750	CH_3COOH	4
B2	1:2:2:0.750		2
B3	1:2:6:0.581		4
B4	1:2:6:0.581		2
B5	1:2:6:0.387		4
B6	1:2:6:0.387		2
C1	1:2;2:0.75	NH_4OH	8
C2	1:2:2:0.75		10
C3	1:2:4:0.194		8
C4	1:2:4:0.194		10
C5	1:2:10:0.194		8
C6	1:2:10:0.194		10
D1	1:2:2:0.75	HCL	4
D2	1:2:2:0.75		2
D3	1:2:6:0.387		4
D4	1:2:6:0.387		2
D5	1:2:10:0.194		4
D6	1:2:10:0.194		2

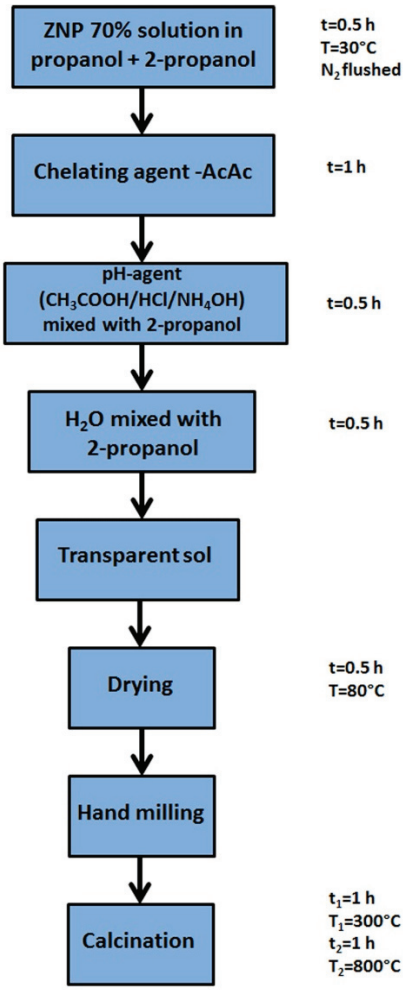

Fig. 1. Powder samples preparation stages

2.2. Characterisation

The thermal properties (TGA/DTA) of the as-obtained powders were studied with a Q 1500D (MOM) derivatograph in static air at a heating rate of 10° min^{-1} in the range 24–1000 °C. X-ray diffraction was performed on a PANalytical X'PERT PRO MPD diffractometer equipped with Cu anode X-ray tube (λ = 0.1540598 nm), Ni filter and RTMS detector

(X'Celerator). The morphology of the dried and calcinated powders was studied the use of scanning electron microscopy (SEM) in a FEI INSPECT S50 microscope. The Particle Size Distribution (PSD) of the samples was measured using a Fritsch Analysette 22 laser analyser.

3. Results

3.1. Synthesis

18 variants of powders with different pH values and pH-agents were prepared by a one-stage sol-gel process. As a comparative sample one variant without the addition of any pH-agent was prepared. The molar ratios and the amount of the chelating agent of all reactants were chosen experimentally, and are the subject of another research. During the synthesis, two types of reaction occurr: hydrolysis and condensation. As a result, a gel is formed. In the ZNP case, during the hydrolysis, the following reaction occurs: $Zr(C_3H_7O)_4 + nH_2O \rightarrow Zr(OH)_n(C_3H_7O)_{4-n} + nC_3H_7OH$. Subsequently, condensation led to the formation of more complicated spatial structures. As a result of the condensation of two hydrolysed metallic centre species, the condensation proceeds with the mechanism of oxolation: $Zr(OH)_n(C_3H_7O)_{4-n} + Zr(OH)_n(C_3H_7O)_{4-n} \rightarrow (OH)_{n-1}(OC_3H_7)_{4-n}Zr\text{-}O\text{-}Zr(C_3H_7)_{4-n}(OH)_{n-1} + H_2O$. In the case where the condensation occurs with one molecule of the hydrolysed metallic centre species and one alkoxide group, the condensation proceeds in accordance with the mechanism of alcoxolation: $Zr(OH)_n(C_3H_7O)_{4-n} + Zr(C_3H_7O)_4 \rightarrow (OH)_{n-1}(OC_3H_7)_{4-n}Zr\text{-}O\text{-}Zr(C_3H_7O)_3 + C_3H_7OH$. As the reaction proceeds, the spatial structure becomes more complicated as a results of hydrolysis and the condensation and creation of a continuous solid gel structure with liquid between the forming clusters. Depending on the pH value, the differences during the preparation of the sol were observed. For the pH range 2–4, the formed gels were characterised almost always by clarity, and there were no major precipitates and in-homogeneity. The as-obtained formed gels had a tendency to relatively large shrinkage during ageing and drying. In colloidal systems with a pH in the range of 8–10, the resulting sols were often two-phase, with a high degree of in-homogeneity and significant numbers of cauliflower-like agglomerates. The pH of the "A" blind-sample was measured and had value oscilating between 6–6.5. Table 2 sets forth selected data collected during the synthesis and formation of the gel.

Table 2. Synthesis observations and results

Sample	Gelation time, h	Gel homogeneity, observations
A	24	Clear, small precipitates
B1	30	Clear, homogeneous
B2	45	Clear, homogeneous
B3	0.1	Clear, small precipitates
B4	0.1	Opaque, medium precipitates
B5	50	Clear, small precipitates
B6	72	Clear, homogeneous
C1	0.05	Clear, small precipitates
C2	0.05	Clear, large precipitates
C3	0.025	Opaque, homogeneous
C4	0.0125	Opaque, large precipitates
C5	0.0125	Opaque, large precipitates
C6	0.0125	Opaque, large precipitates
D1	0.33	Clear, homogeneous
D2	18	Clear homogeneous,
D3	0.0125	Clear homogeneous,
D4	0.0125	Clear, small precipitates
D5	0.0125	Clear, medium precipitates
D6	0.0125	Clear, medium precipitates

3.2. Thermal studies

The effect of pH and pH-agent on the thermal behaviour during calcination was investigated. The aim was to trace their correlation with the occurrence of thermal transformations and possible phase transitions and the stability of AcAc with ZNP and the selection of the optimum calcination temperature. Based on the results of the thermal analysis, some samples were chosen for further study. From all the samples, the most characteristic and reproducible TGA curves were

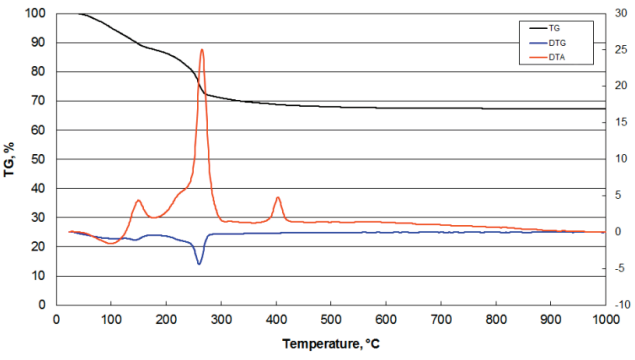

Fig. 2. TG, DTG, DTA curves of reference powder sample only with AcAc

selected for thermal powders from each powder group. Figure 2 shows a sample of the curves of the "A" sample obtained only using AcAc without the addition of any pH-agent. The average weight loss during the analysis was as follows: "B"-series 32.3%, "C"-series 25.0% and "D"-series 26.5%. In contrast, sample 'A' weight loss was approximately 32%. The samples selected for the next study were characterised by the lowest shrinkage from each of the groups: B1 – 25%, C5 – 15%, D3 – 18% and D5 – 16% (Fig. 3a, b, Fig. 4a, b). The shrinkage of the each sample is equal to or less than 25%, which is within the range dedicated to the sintering and milling procedure for dental zirconia [23].

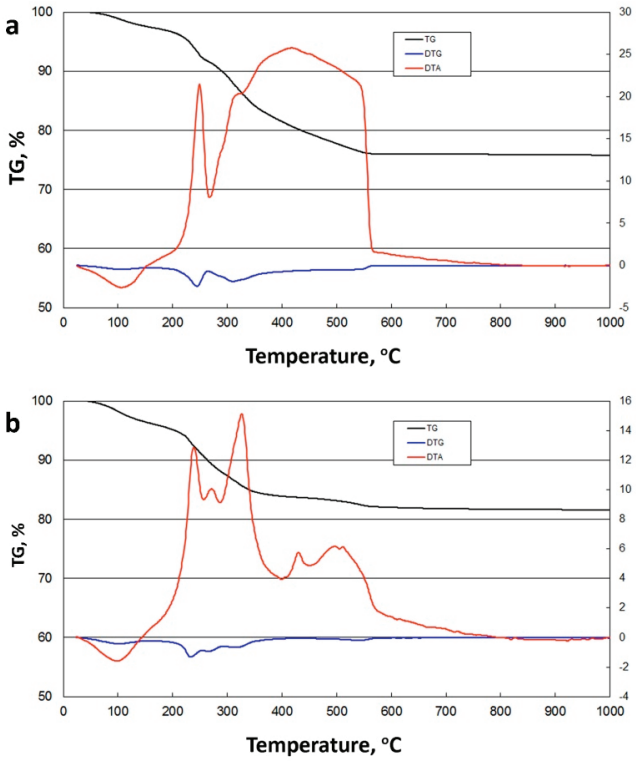

Fig. 3. Thermal analysis curves for samples: a) B1, b) D3

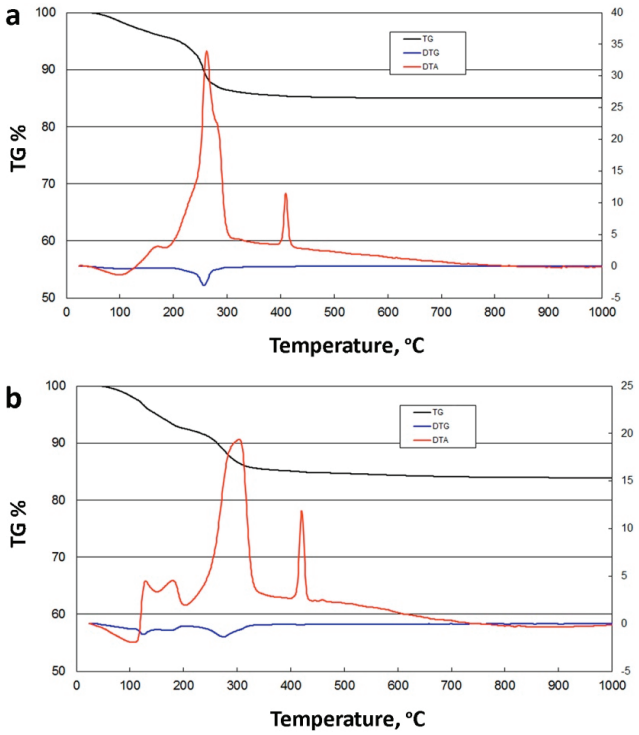

Fig. 4. Thermal analysis curves for samples: a) C5, b) D5

3.3. XRD studies

X-ray patterns of the obtained powder samples are presented in Fig. 5. It is visible that all compared samples differ in quantitative phase composition (i.e., diffraction lines intensity), as well as diffraction lines broadening. The results of quantitative phase composition determination by the Rietveld refinement method are presented in Table 3. The results of crystallite size and lattice strain calculated based on the Scherrer equation are presented in Table 4. Crystal lattice parameters determined during Rietveld refinement and the calculated crystal lattice volumes are presented in Table 4.

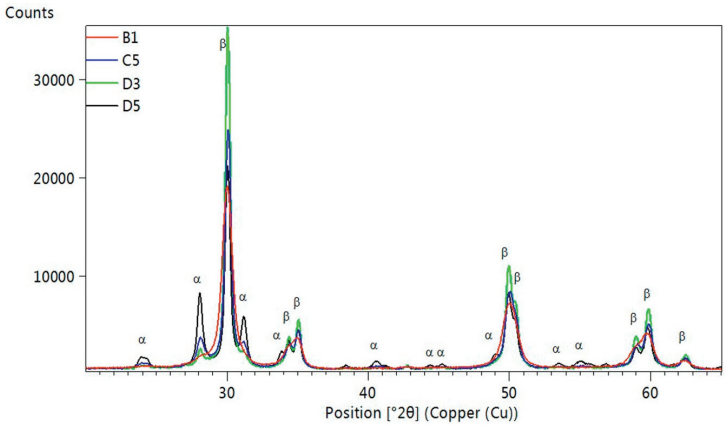

Fig. 5. X-ray pattern of B1, C5, D3 and D5 samples

Table 3. Crystallites size and lattice strain of B1, C5, D3 and D5 powders

Sample	Phase	Crystallite size [Å]	Lattice strain [%]
B1	β-ZrO_2	119	1.28
	α-ZrO_2	62*	?
C5	β-ZrO_2	233	0.72
	α-ZrO_2	150	1.12
D3	β-ZrO_2	295	0.59
	α-ZrO_2	157	1.07
D5	β-ZrO_2	299	0.59
	α-ZrO_2	247	0.73

* approximate value (FWHM hard to determination due to peaks overlaps, see Fig. 5).

Table 4. Crystal lattice parameters and volumes of B1, C5, D3 and D5 powders

Sample	Phase	a_0 [Å]	b_0 [Å]	c_0 [Å]	β [°]	V [Å^3]
B1	β-ZrO_2	3.6194		5.2115		68.28
	α-ZrO_2	5.2736	5.2240	5.2233	98.172	142.44
C5	β-ZrO_2	3.6160		5.2040		68.04
	α-ZrO_2	5.1773	5.2156	5.3487	98.669	142.78
D3	β-ZrO_2	3.6150		5.2082		68.06
	α-ZrO_2	5.1754	5.2156	5.3457	98.703	142.63
D5	β-ZrO_2	3.6163		5.2078		68.11
	α-ZrO_2	5.1816	5.2184	5.3547	98.830	143.07

3.4. SEM

Based on the SEM microphotograph observation, the difference between the prepared powders could be evaluated. Fig. 6a–c shows a comparison of the powders from all three groups after drying. Fig. 7a–c shows these same powders after calcination. Powders from series "B" (Fig. 6a, Fig. 7 a) pH 2–4 were character-

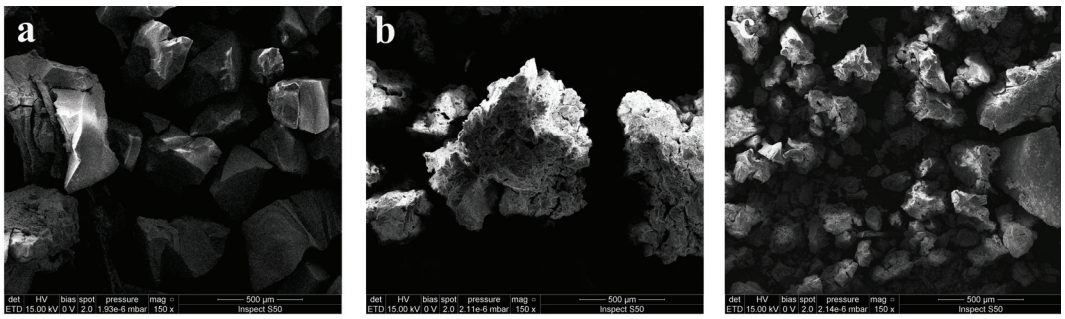

Fig. 6. SEM microphotographs of the as-dried powders: a) B1, b) C5, c) D5

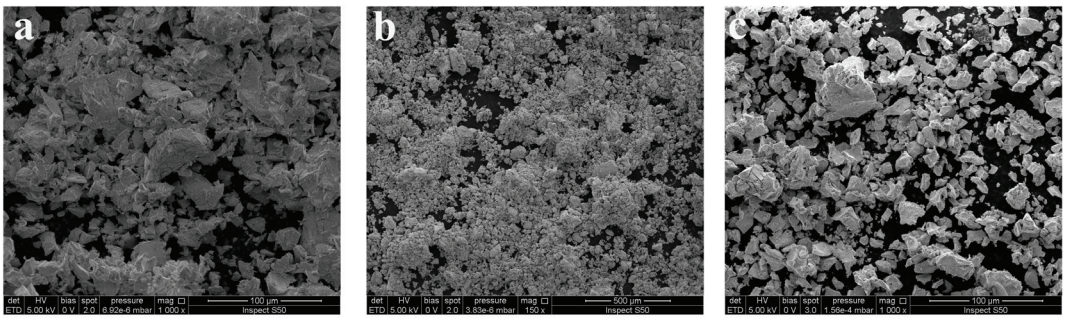

Fig. 7. SEM microphotographs of the calcined at 800 °C powders a) B1, b) C5, c) D5

ised by the relatively large size of the grains in the range dozens of micrometers they were so quite hard that they were hard to crush with a mortar and pestle. The obtained powders were solid, hard to disintegrate with a poor degree of agglomeration. In contrast, for the "C"-series (Fig. 6b, Fig. 7b), the obtained powders were characterised by a smaller grain size in a range of few microns, and a high degree of agglomeration. The powders (Fig. 6c, Fig. 7c) very easily disintegrated, even by touching.

3.5. Particle Size distribution

In Fig. 8, the PSDs of investigated samples are presented. In the case of B1 sample, the mean diameter value d_{43} was equal to 24.95 µm. The unimodal distribution had the dominant value for the 15.90–18.30 µm particle size class and the largest particles encountered had a size of about 200 µm. Similar results were obtained for D5 sample, for which the modal range was identical. On the other hand, the mean particle size was smaller (d_{43} = 17.19 µm), which resulted from a narrower particle size distribution. In this case, the largest particles had a size no larger than 70 µm. The C5 sample was the only one with a bimodal particle size distribution with modes located at 21.06–24.24 µm and 64.84–74.62 µm size classes. The d_{43} diameter was equal to 49.88 µm. The largest particles had a size equal to 350 µm. Finally, D3 sample had the broadest range of particle sizes, exceeding the measurement capabilities of the laser sizer. The largest particles had diameters above 1 mm and could be easily distinguished with the naked eye. In this case, the d_{43} was equal to 99.04 µm, however, this value should be understood as "at least as large as". The mode was obtained for the 27.90–32.11 µm size class. It has to be emphasised that in each case the submicron particles were present in the suspension. In the case of B1, C5 and D5 samples, their cumulative volume fraction was close to 3.3%, whereas in the case of D3 sample, this value was three times lower. Another interesting fact is that in all the cases the mode locations lie in a narrow range of particle sizes between 15.90–32.11 µm (the first mode in the case of the C5 sample).

4. Discussion

4.1. Synthesis

For the "B" series powders, which used CH_3COOH as a pH-agent, the following relationships were observed:

- Powders B1, B2, compared to A1 sample, use more acid pH, triggering the smaller, loosely connected aggregates, which was especially visible for B2 and pH 2;
- Powders B3 and B4 have a greater concentration of agglomerates;
- Powders B5 and B6 present a lower concentration of large, loosely-bound agglomerates that can be observed macroscopically for the presence of both agglomerates and aggregates.

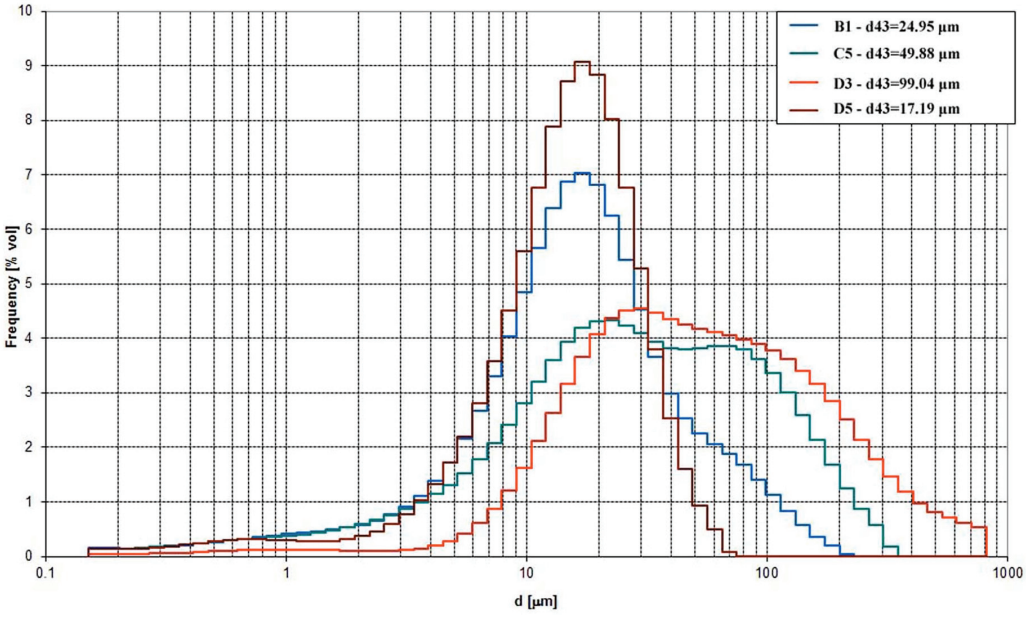

Fig. 8. PSDs of investigated samples B1, C5, D3 and D5

For the powders from the "C" series, obtained with NH_4OH, the following relationships were observed:

- powders C1 and C2 were independent of the pH value, and characterised by the occurrence of large quantities of solid, hard aggregates, compared to A1;
- powders C3 and C4 were characterised by a "transient" morphology (we observed a large number of loosely bound agglomerates, aggregates and hard aggregates); no pH value influence was observed;
- C5 and C6 powders were characterised by the highest number of irregular, large, loosely bound agglomerates, as in the remaining samples, the series of "C" macroscopically observed pH effect was negligible.

For powders of the "D" series, which used HCl, we observed almost the same changes as for the "B" series. Noted differences relate to the forms of the aggregate samples D1 and D2. The observed aggregates have a reproducible morphology and the shape of individual grains close to pyramidal.

4.2. Thermal properties

For the "A" powder (Fig. 2), the TGA curve show four characteristic peaks: endothermic associated with the evaporation of water at 67–110 °C; exothermic at 145 °C, associated with the disintegration of propanol; exothermic at 264 °C, associated with the disintegration of AcAc [12], [22]; and a small exothermic peak at 410 °C that we expected came from crystallisation of a new phase. For sample C5, the situation is almost similar. The peak probably responsible for the crystallisation of a new phase is much sharper also in D5 sample. In contrast, for samples B1, D3 and D5, the interpretation was more sophisticated. For B1 three peaks were found: endothermic at 86–120 °C, associated with the evaporation of water; exothermic at approximately 250 °C, associated with the collapse of propanol; and a large, broad exothermic hump between 263–562 °C, which is associated with decomposition of AcAc. All energy effects in B1 are shifted to the right of the plot due to a significant molar ratio of AcAc (ZNP: AcAc, 1: 0.75), which consequently formed a thermally more stable complex, where decomposition occurs in a higher temperature range compared to the "A" sample. For both powders from the "D"-series, we observed characteristic peaks of water evaporation and disintegration of organic spacies. The fact that there are two peaks in the range ~390–560 °C in sample D3, and a very sharp peak at about 417 °C for sample D5, is striking. This situation cannot be associated only with the decomposition of organic compounds: it is, therefore, very likely that the signals came from the ZrO_2 phases [24].

4.3. Phase composition

Sample D3 contains the highest amount of tetragonal (β) phase 86.8 wt.%. The sample from the same series D5 has smallest tetragonal phase concentration among all those tested (53.4 wt.%). Sample B1 has the smallest average crystallite size and largest lattice strain of tetragonal phases among all tested samples. This suggests that the crystals in B1 powder contain the greatest amount of wide-angle boundaries and other crystal defects that influence their properties. Samples D3 and D5 have the largest crystallite size (about 300 Å) and the smallest lattice strain (0.59%) amongst all tested samples, suggesting a lower number of crystal defects compared to sample C5 and, especially, B1.

4.4. Morphology

Using pH in the range 2–4, it is possible to obtain powders hard to mill mechanically. In contrast, grain size observed was a smaller, measured during PSD measurement than powders of the "C" series, characterised by very good mechanical disintegration. For the pH range of 8–10, larger grains with a bimodal particle size distribution in two narrow range grain sizes were obtained. However, comparison of the SEM microphotographs clearly shows the visible C5 multi-grain large agglomerates, which can be further ground. By contrast, grains in samples B1 and D5 have more or less large solid crystals. This situation can be explained by the fact of the occurance of very instant hydrolysis and condensation after the addition of NH_4OH and the accompanying formation of large multi-aggregates during the sol-gel process. As a result of hydrolysis catalysed with NH_4OH, a large number of aggregates was formed with a tendency to clump together into larger complexes that are already visible with the naked eye in the synthesis. In contrast, synthesis with the addition of CH_3COOH and HCL as a catalyst proceeded much more smoothly. The resulting sols may be divided into smaller aggregates and usually are reasonably homogeneous sols. What is clear is that the addition of NH_4OH accelerated the hydrolysis rate more significantly, leading to the formation of aggregates in calcined powders. The morphology of the powders obtained in the series of "C"

corresponds to the so-called *soft agglomerates* described by [19]. The use of such powders for the preparation of green-bodies allows for the solid ceramic without adversely participate pores. In contrast, for powders with group "B", their morphology is similar to the so-called *hard-agglomerates* that are conducive to the formation of pores in the preparation of green-bodies, hindering densification under sintering.

5. Conclusions

Compared to neutral pH used in earlier studies (pH = 6.5–7) [21], the change to acidic (pH = 2–4) or alkaline (pH = 8–10) caused an increase in the thermal stability of the complex AcAc-ZrOPr, which contributed to an increase in mass loss of the calcined powders. On the basis of measurements of the particle size distribution (PSD), the relation between the occurrence of agglomeration and the pH was shown. pH variation from neutral to acidic resulted in weakening of the intermolecular interactions, thus allowing us to obtain a smaller grain size of the powders after calcination; for powders prepared with alkaline pH, the PSD obtained too little information. Based on the SEM results, the correlation between the pH of the colloidal and obtainable morphology of ceramic powders was shown that the use of pH = 8 caused large clusters of loosely coupled agglomerates. The data obtained of the morphology of our powders are in good agreement with the results of Caruso et al. [16].

Unfortunately, the analysis of the phase composition (XRD) cannot bring about the correlation between pH and the resulting phase composition. In this matter, further research is still needed.

On the basis of the information obtained, there may be a need for selection and optimisation methods between stage grinding of the powders obtained using the aforementioned method.

References

[1] AMARAL M., VALANDRO L.F., BOTTINO M.A., SOUZA R.O.A., *Low-temperature degradation of a Y-TZP ceramic after surface treatments*, J. Biomed. Mater., Research Part B: App. Biomater., 2013, 101, 1387–1392.

[2] BASU B., VLEUGELS J., VAN DER BIEST O., *Transformation behavior of tetragonal zirconia: role of dopant content and distribution*, Mater. Sci. Eng., 2004, A366, 338–347.

[3] CHEVALIER J., GREMILLARD L., VIRKAR A.V., CLARKE D.R., *The tetragonal-monoclinic transformation in zirconia: lessons learned and future trends*, J. Am. Ceram. Soc., 2009, 92, 9, 1901–1920.

[4] DASARI H.P., AHN J.S., AHN K., PARK S.Y., HONG J., KIM H., YOON K.J., SON J.W., LEE H.W., LEE J.H., *Synthesis, sintering and conductivity behavior of ceria-doped Scandia-stabilized zirconia*, Sol. State Ion., 2014, 264, 103–109.

[5] CALLON G.J., GOLDIE D.M., DIBB M.F., CAIRNS J.A., *X-ray diffraction analysis of yttria stabilized zirconia powders by an organic sol-gel method*, J. Mater. Sci. Lett., 2000, 19, 1689–1691.

[6] FABBRI P., PICONI C., BURRESI E., MAGANAMI G., MAZZANTI G., MINGAZZINI C., *Liftime estimation of a zirconia-alumina composite for biomedical applications*, Dent. Mater., 2014, 30, 138–142.

[7] GREMILLARD L. et al., *Degradation of implant meterials*, [in:] *Degradation of implant meterials* (ed. N. Eliaz), Springer, New York 2012, 195–240.

[8] GUO X., *Property degradation of tetragonal zirconia induced by low-temperature defect reaction with water molecules*, Chem. Mater., 2004, 16, 3988–3994.

[9] GUO X., ZHANG Z., *Grain size dependent grain boundary defect structure: case of doped zirconia*, Acta Mater., 2003, 51, 2539–2547.

[10] HALLMANN L., ULMER P., REUSSER E., LOUVEL M., HÄMMERLE Ch.H.F., *Effect of dopants and sintering temperature on microstructure and low temperature degradation of dental Y-TZP-zirconia*, J. Eur. Ceram. Soc., 2012, 32, 4091–4104. (13)

[11] HUANG W., YANG J., WANG CH., ZOU B., MENG X., WANG Y., CAO X., WANG Z., *Effects of Zr/Ce molar ratio and water content on thermal stability and structure of ZrO_2-CeO_2 mixed oxide prepared via sol-gel process*, Mater. Res. Bull, 2012, 47, 2349–2356.

[12] INOKOSHI M., ZHANG F., DE MUNCK J., MINAKUCHI S., NAERT I., VLEUGELS J., VAN MEERBEEK B., VANMEENSEL K., *Influence of sintering conditions on low-temperature degradation of dental zirconia*, Dent. Mater., 2014, 30, 669–678.

[13] KELLY J.R, DENRY I., *Stabilized zirconia as a structural ceramic: An overwiew*, Dent. Mater, 2008, 24, 289–298.

[14] KEUPER M., BERTHOLD CH., NICKEL K.G., *Long-time aging in 3 mol.% yttria-stabilized tetragonal zirconia polycrystals at human body temperature*, Acta Biomater., 2014, 10, 951–959.

[15] MÁLEK J., *The applicability of Johnson–Mehl–Avrami model in thermal analysis of the crystallization kinetics of glasses*, Themochem. Acta, 1995, 267, 61–73.

[16] MAMANA N., DÍAZ-PARRALEJO A., ORTIZ L., BAJO S., CARUSO R., *Influence of the synthesis proces on the features of Y_2O_3-stabilized ZrO_2 powders obtained by the sol-gel method*, Ceram. Int., 2014, 40, 6421–6426.

[17] MIYAZAKI T., NAKAMURA T., MATSUMURA H., BAN S., KOBAYASHI T., *Review: Current status of zirconia restoration*, J. Prost. Res., 2013, 57, 236–261.

[18] MORRISSEY A., TONG J., GORMAN B.P., REIMANIS I.E., *Characterization of nickel ions in nickel-doped yttria-stabilized zirconia*, J. Am. Ceram. Soc., 2014, 97(4), 1041–1047.

[19] MORTEZA HAJIZADEH-OGHAZ, REZA SHOJA RAZAVI, ALI GHASEMI, *The effect of solution pH value on the morphology of Ceria-Yttria co stabilized zirconia particles prepared using the polymerizable complex method*, J. Clust. Sci., 2016, 27, 469–483.

[20] NAKONIECZNY D., WALKE W., MAJEWSKA J., PASZENDA Z., *Characterization of magnesia-doped yttria-stabilized zir-*

conia powders for dental technology applications, Acta of Bioeng. Biomech., 2014, 16(4), 99–106.

[21] NAKONIECZNY D., PASZENDA Z., DREWNIAK S., RADKO T., LIS M., *ZrO_2-CeO_2 ceramic powders obtained from a sol-gel process using acetylacetone as a chelating agent for potential application in prosthetic dentistry*, Acta of Bioeng. Biomech. accepted to print. 2016, 3(18).

[22] NAUMENKO A., GNATIUK I., SMIRNOVA N., EREMENKO A., *Characterization of sol-gel derived TiO_2/ZrO_2 films and powders by Raman spectroscopy*, Thin Solid Films, 2012, 520, 4541–4546.

[23] TANAKA S., TAKABA M., ISHIURA Y., KAMIMURA E., BABA K., *A 3-year follow-up of ceria-stabilized zirconia/alumina nanocomposites (Ce-TZP/A) frameworks for fixed dental prostheses*, J. Prost. Res., 2015, 59, 55–61.

[24] STOIA M., BARVINSCHI P., BARBU-TUDORAN L., NEGREA A., BARVINSCHI F., *Influence of thermal treatment on the formation of zirconia nnaostructured powder by thermal decomposition of different precursors*, J. Cryst. Growth, 2013, 381, 93–99.

[25] WOJDA S., SZOKA B., SAJEWICZ E., *Tribological characteristics of enamel-dental material contacts investigeted in vitro*, Acta of Bioeng. Biomech, 2015, 17(1), 21–29.